Enhanced photoluminescence from porous silicon formed by nonstandard preparation

A. I. Belogorokhov, R. Enderlein, A. Tabata, and J. R. Leite
Instituto de Física, Universidade de São Paulo, Caixa Postal 66318, 05315-970 São Paulo, SP, Brazil

V. A. Karavanskii and L. I. Belogorokhova
Department of Physics, Moscow State University, Leninsky Gory, Moscow 119899, Russia
(Received 3 April 1997)

Using a nonstandard preparation procedure, porous silicon (PS) samples are grown whose overall photoluminescence (PL) intensities exceed those of standard PS samples from the same Si wafer up to 50 times, and whose PL maxima occur in the high-energy range at about 1.8 eV. The preparation includes an electrochemical etching step in a HCl:HF:C_2H_5OH electrolyte solution with varying HCl contents. The fine structure of low-temperature PL spectra is discussed in terms of the confinement model. Crystalline silicon wires are identified as PL active structural elements, and the wire diameters are determined. At room temperature, four broad PL peaks are observed. The evolution of these peaks with varying HCl content of the electrolyte provides detailed insight into the porous structure of the samples. PL studies on laser-irradiated samples indicate that the Si wires are covered by stoichiometric silicon oxide. We conclude that the absence of Si dangling bonds, and the well-ordered wire structure, could be responsible for the enhanced PL intensity of our PS samples, as well as for their stability against exposition to air and postanodization. [S0163-1829(97)08139-3]

I. INTRODUCTION

Porous silicon (PS) forms a new kind of nanometer material with light emission in the visible spectral range. It has been widely investigated by experimental and theoretical means during the past six years. The photoluminescence (PL) of PS is believed to be mainly due to quantum size effects,[1–6] although the existing data and their interpretations are still controversial.[7–9,6] While there seems to be clear evidence that light emission originates from Si crystallites,[10,6] the difference of only 0.3 eV between the red PL peak and the fundamental band gap of Si, as well as the effect of chemical treatment[11–13] on the PL spectra, indicate that the radiation process is more complex than the simple confinement picture suggests. Moreover, the PL properties depend on the PS microstructure and the surface chemical composition of the porous material. These observations have stimulated alternative explanations like, for example, models which assume siloxene molecules[14] or nonbridging-oxygen-hole complexes[15] as light emitting entities. A critical review of these and other models, combined with a further elaboration of the confinement model, have recently been given in Ref. 6.

Owing to the dependence of the PL properties on the PS microstructure, one should be able to prepare porous silicon samples of enhanced PL emission and improved crystalline stability by changing the chemical composition of the internal PS surface. This may be attempted in two different ways, either *during* preparation as, for example, by varying the current density, or *after* preparation, by prolonged chemical treatment in a solution or in a gaseous mixture of etchants. In this paper, we employ the first way. We modify the chemical nature of the nanocrystallite surfaces by using an electrolyte of nonstandard composition, i.e., a HCl:HF:C_2H_5OH solution of varying HCl content. It turns out that samples prepared by means of this electrolyte exhibit considerably better PL properties than samples obtained by means of the standard procedure. The changes of the PL spectra are studied in detail in dependence on the preparation conditions. With increasing HCl content of the electrolyte the spongelike PS structure transforms into a wirelike structure. The PL spectra of laser irradiated PS samples are interpreted in light of the quantum confinement model to infer details of surface chemical composition and structure of the PS wires. We conclude that the absence of nonstoichiometrical silicon oxide, and the well-ordered wire structure, could be the reason for the improved PL properties of PS samples prepared under the nonstandard conditions.

The paper is organized as follows. In Sec. II we describe the sample preparation and the experimental PL setup. The PL spectra are presented and analyzed in Sec. III. Temporal changes of the PS samples under laser irradiation are studied in Sec. IV. Section V concludes the paper.

II. SAMPLE PREPARATION AND EXPERIMENTAL SETUP

All PS samples are made from (100) oriented, mirror-polished boron-doped p-type CZ silicon substrate wafers of 10–12 Ω cm resistivity and a thickness of 300 μm. Commonly, the Si wafer is anodically etched for 20 min in an electrolyte containing a 1:1 mixture of methanol and 49% hydrofluoric acid, using a current density of 30 mA cm^{-2} (standard procedure). An electrochemical cell with platinum electrodes is used for the anodization. In our nonstandard procedure, the wafers are electrochemically etched in an HCl:HF:C_2H_5OH electrolyte at a current density of 30 mA cm^{-2}, and anodized for 20 min. The HCl content of the electrolyte is varied in our experiments, it was 5% for sample $A1$, 10% for sample $A2$, 20% for sample $A3$, and

40% for sample $A4$. Samples prepared by the standard procedure are referred to as $A0$.

The thicknesses of the porous layers were measured by optical microscopy. They were found to range between 15 and 20 μm. The porosity was more than 70%, as estimated by the gravimetric method. Experimental data on the microstructure of the porous layers and their surface morphology were obtained by means of a scanning electron microscope JEOL 840A equipped with a Link system. Sample $A0$ prepared by the standard procedure exhibits the well-known spongelike structure. The spongy PS consists of many randomly distributed and interconnected pores. For sample $A1$ obtained by the nonstandard procedure with a low (5%) HCl content, we find a thin layer with wirelike crystallites aligned perpendicular to the (100) surface on top of a still existing spongelike interfacial layer. The thickness of the wirelike layer increases, and the thickness of the spongelike layer decreases if the HCl content is increased as is done in preparing samples $A1-A4$.

The PL measurements were performed with a SPEX 1702/04 spectrometer using the 488 nm and 514.5 nm lines of an Ar^+ laser (Innova 90) as excitation source. The luminescence radiation from the samples was focused on the slit of a monochromator and the intensity was measured with a GaAs photomultiplier. The irradiation power was in the range of 0.5–100 mW and was focused at an area of about 1 mm^2. In all measurements the laser power was monitored, and the same geometric conditions were used in order to have comparable data. The sample was kept in air during the measurements. The PL spectra were taken from different sites of the sample to avoid the influence of laser irradiation on the structure of the measured sample region. The scanning time of every PL spectrum was 3 min.

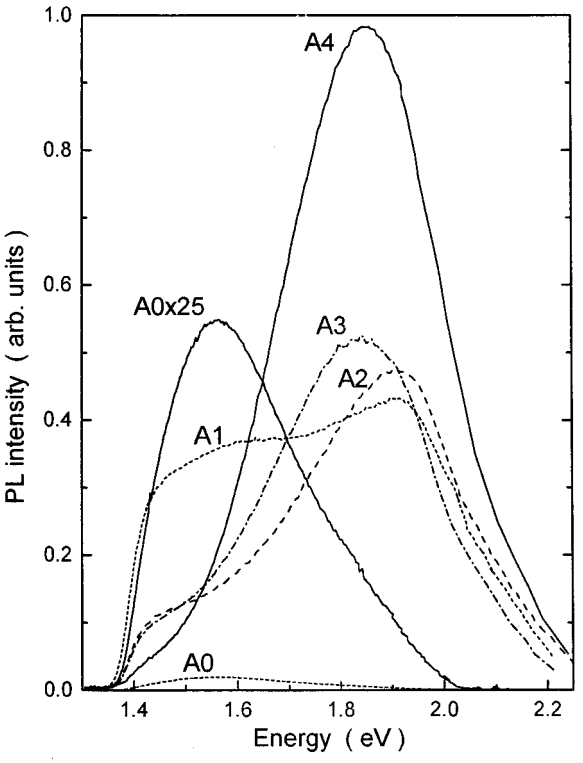

FIG. 1. PL spectra obtained at room temperature from samples $A0-A4$. Excitation wavelength and power are 488 nm and 50 mW, respectively. Spectrum of sample $A0$ multiplied by a factor of 25.

III. PL SPECTRA AND PS MICROSTRUCTURE

A. Overall comparison of PL spectra from differently prepared samples

Figure 1 shows the PL spectra of various samples taken at room temperature. The overall PL intensities of samples $A1$ to $A4$, prepared by the nonstandard procedure, are up to 50 times larger than the overall PL intensity of sample $A0$ prepared in the standard way. The PL peak of sample $A0$ occurs at lower energies than the peaks of samples $A1$ to $A4$. With increasing HCl content of the electrolyte, the PL peaks of samples $A1$ to $A4$ undergo a blueshift, and simultaneously their heights increase. For sample $A4$ one has a single PL peak of Gaussian shape, while the PL line shapes of samples $A1$, $A2$, and $A3$ cannot be described in terms of a single peak.

B. Fine structure of low-temperature PL spectra and PL active structural elements

Figure 2 shows the PL spectra of samples $A1-A4$ recorded at $T=1.4$ K. They exhibit a fine structure consisting of a set of small peaks spaced almost equally by 17–21 meV. In the quantum confinement model, these peaks may be attributed to silicon wires or dots of different diameters.[16–18] In the case of wires, calculations based on a variational envelope function approach[16] predict a $d_{\rm wire}^{-1.39}$ dependence of the optical gap on the wire diameter $d_{\rm wire}$. Other calculations using linear combinations of atomic orbitals give similar results.[17] These theoretical findings are reproduced in Fig. 3. Also shown in this figure are calculated gaps for spherical quantum dots as a function of their diameter $d_{\rm dot}$.[18] The variation of the gap with $d_{\rm dot}$ follows almost the same power law which applies in the case of wires, i.e., $d_{\rm dot}^{-1.39}$. The gap-versus-diameter curves of Fig. 3 are used to analyze the PL spectra of Fig. 2.

Let us first suppose the PL active structural elements of the PS samples to be wires. Because of the (100) substrate orientation it is natural to assume that the wires are aligned along the cubic crystal axis [100]. The wire diameters $d_{\rm wire}$ may only change in steps $\Delta d_{\rm wire}$ given by the average projection of the nearest neighbor vector $(a/4)(1,1,1)$ into the (100) plane (a—lattice constant). One has $\Delta d_{\rm wire}=[(1+\sqrt{2})/2]\times(a/4)=0.302\times a$. Hence, the possible wire diameters are $d_{\rm wire}=\overline{d_{\rm wire}}+k\times 0.302\times a$ where k means an (positive or negative) integer and $\overline{d_{\rm wire}}$ the average wire diameter. Let $\hbar\nu$ be the PL peak position for a wire of the average diameter $\overline{d_{\rm wire}}$. Then, assuming $\overline{d_{\rm wire}}\gg\Delta d_{\rm wire}$, a wire of diameter $\overline{d_{\rm wire}}+k\Delta d_{\rm wire}$ leads to a PL peak at $\hbar\nu=\overline{\hbar\nu}+\Delta\hbar\nu_k$, where[19]

$$\frac{\Delta\hbar\nu_k}{\overline{\hbar\nu}}=-1.39k\,\frac{\Delta d_{\rm wire}}{\overline{d_{\rm wire}}}. \tag{1}$$

The same consideration may be applied under the assumption that the light emitting elements of the PL samples are spherical dots rather than wires. In a [100] direction, the dot

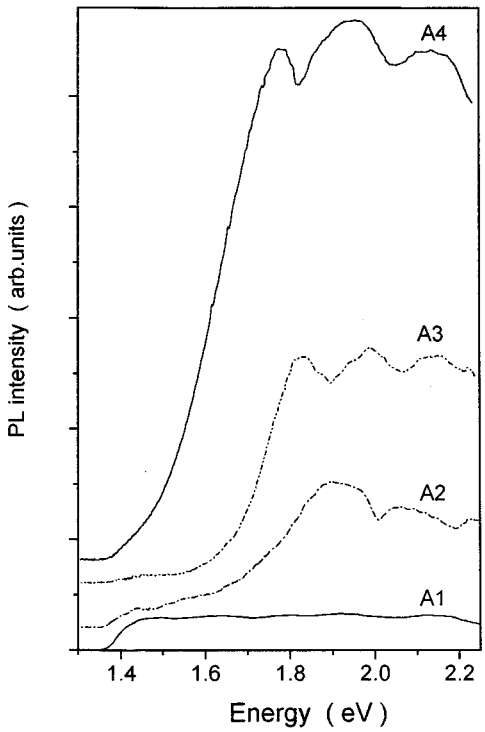

FIG. 2. PL spectra of samples $A1-A4$ taken at $T=1.4$ K. Excitation wavelength and power as in Fig. 1.

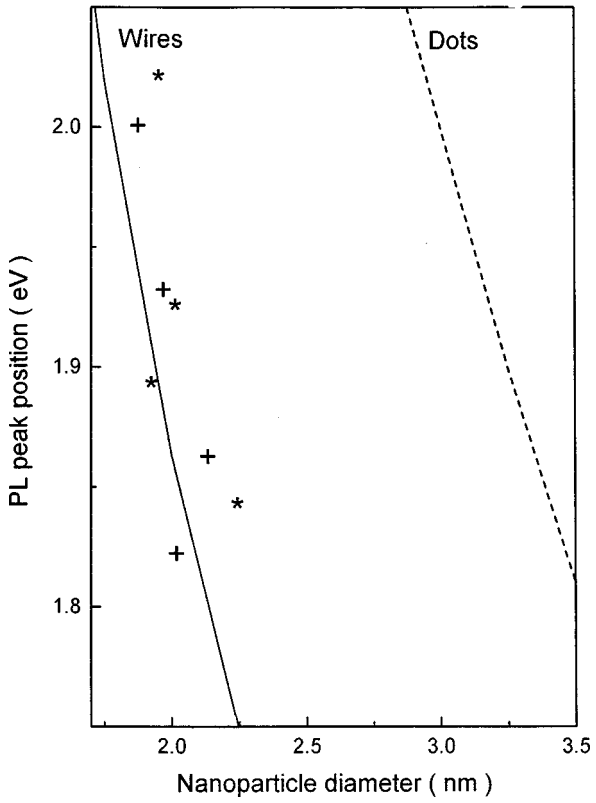

FIG. 3. Dependence of PL peak position on nanoparticle diameter. The solid and dashed lines are theoretical predictions for the energy gaps of crystalline Si quantum wires and dots, respectively. The experimental results are taken from the PL spectra at 1.4 K (*) and 295 K (+).

diameters d_{dot} may only change in steps of $(a/4)$, and in a [111] direction the possible changes are by a factor of $\sqrt{3}$ larger. Averaging over all directions, we obtain an average step Δd_{dot} for the dot diameter changes equal to $(1/7)(3\times 1+4\times\sqrt{3})(a/4)=0.355\times a$. The PL spectra of the various samples (only part of them are shown in Fig. 2) deliver experimental values for $\overline{\hbar\nu}$ and $\Delta\hbar\nu_k$. Using these values in Eq. (1), one obtains average wire diameters $\overline{d_{\mathrm{wire}}}$ for the various samples, provided that wires are in fact their PL active structural elements. The thus obtained average diameters $\overline{d_{\mathrm{wire}}}$ combined with the pertinent average peak positions $\hbar\nu$ are plotted in Fig. 3 as experimental points. Since relation (1) also applies to dots, we may derive average dot diameters as well. These are by a factor of 1.18 larger than the average wire diameters for the same sample. To avoid confusion, the $(\overline{d_{\mathrm{dot}}},\overline{\hbar\nu})$ points are not plotted in Fig. 3. It is anyway clear that these points are far left of the theoretical curve for dots, so that dots may be excluded as light emitting structural elements of our PL samples. On the other hand, the experimental points are close to the theoretical curve for wires. This implies that, on the assumption that the confinement model is valid, wires should be the PL active components.

C. Line shape analysis of high-temperature PL spectra

In the high-temperature spectra, wires of diameters fluctuating by atomic steps around a certain average diameter give rise to one broad peak of Gaussian shape. If several peaks are seen in the experimental high-temperature PL spectra, the presence of wire groups of considerably different average diameters is indicated, each group giving rise to its own Gaussian peak. Inspecting Fig. 1, one notices that the PL spectra of samples $A1$, $A2$, and $A3$, in fact, resemble a multipeak behavior. In Fig. 4 we show the decomposition of the $A1$ spectrum into four Gaussian peaks, labeled as a,b,c,d. Such a decomposition has been made for the spectra of all samples in Fig. 1. The results are shown in Figs. 5–8. Figure 5 shows the positions of peaks a, b, c, and d as a sample function, more strictly speaking, as a function of the HCl content of the electrolyte used for the sample preparation. Peak a is the only spectral feature for the standard sample $A0$, while all nonstandard samples exhibit four peaks. This indicates that peak a is due to the spongelike layer, which forms the only porous region in sample $A0$, while peaks b, c, and d may be attributed to the wirelike layers containing wires of different diameters. Increasing the HCl content, peak a stays almost constant, while peaks b, c, and d shift to higher energies. At the same time, the distances between peaks b, c, and d decrease with growing HCl content, ending up at almost zero distances for high HCl content. Using the average-peak-position versus average-diameter plot of Fig. 3, we may associate each peak position with a wire group of a certain average diameter. The change of the average wire diameters with HCl content of the electrolyte is shown in Fig. 6. In Fig. 7, the peak heights are plotted versus HCl content. One observes a shrinkage of peak a by more than two orders of magnitude changing the HCl content from 0% to 40%.

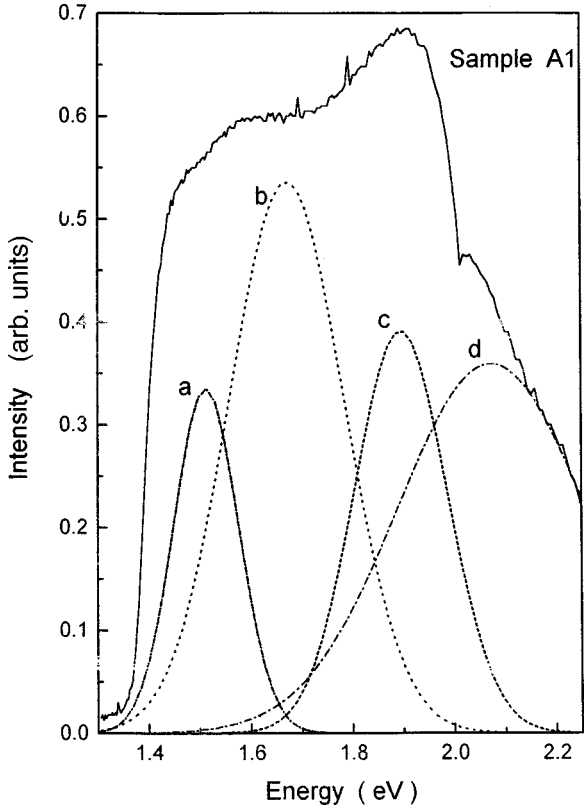

FIG. 4. Fit of the experimental PL spectrum for sample $A1$ to a sum of four Gaussians, labeled as a,b,c,d. Excitation wavelength and power as in Fig. 1. $T=295$ K.

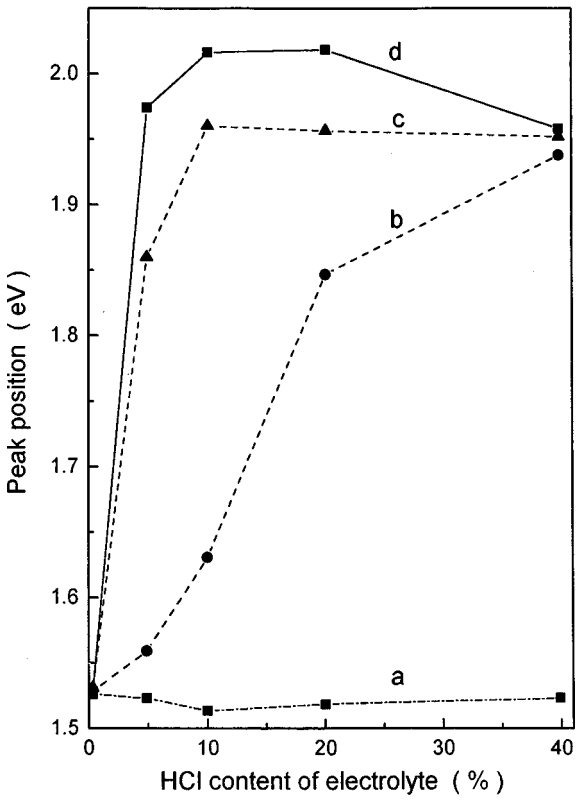

FIG. 5. PL peak positions of samples $A0-A4$ prepared by means of electrolytes of different HCl contents. $T=295$ K.

The reason for this decrease follows quite naturally from the interpretation of peak a as being due to the spongelike layer: The thickness of this layer decreases with raising HCl content. That peaks c and d rapidly grow, whereas peak b rapidly shrinks with increasing HCl content, can also be easily explained in our structural model of the porous layers: the fraction of wires with small diameters becomes larger, and that with large diameters becomes smaller if the HCl content increases. Finally, in Fig. 8, the variation of the linewidth [full width at half maximum (FMHW)] of the four peaks is shown as a function of the HCl content of the electrolyte. All peaks become narrower with increasing HCl content, indicating the smaller dispersion of wire diameters within each wire group.

Concerning the stability of the samples against degradation it should be mentioned that, prior to the PL measurements reported above, all samples were exposed to air for a period of 9 months. Some of the samples had also been measured immediately after preparation. The spectra were exactly the same as those reported above.

IV. STRUCTURAL STABILITY OF PS SAMPLES UNDER LASER IRRADIATION

Recently, the influence of laser irradiation on PL and Raman spectra of PS samples prepared by the standard anodization procedure in an HF:$C_2H_5OH=2:1$ electrolyte has been investigated.[23] In the initial stage of the irradiation, the Raman and PL peaks showed a similar oscillatory behavior as the nonirradiated samples. After some time (typically 50 minutes) both the PL and Raman peaks were shifted to higher energies, and finally these peaks remained unchanged while continuing the laser exposition. The authors of Ref. 23 attributed this behavior to the laser-induced oxidation and

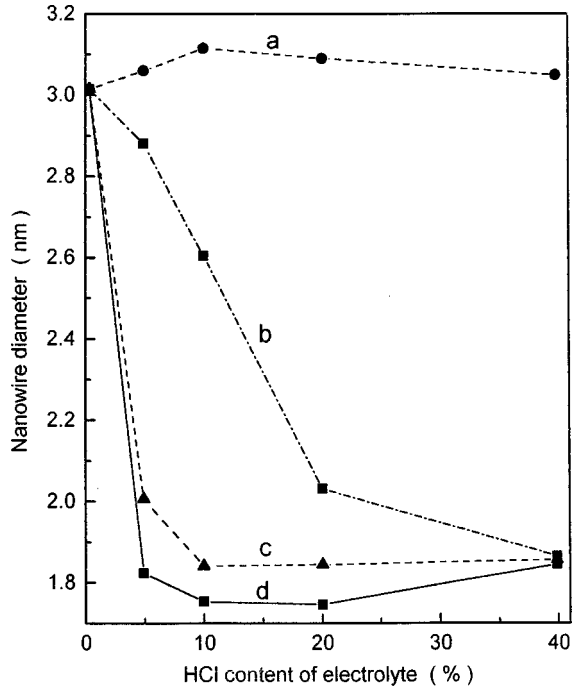

FIG. 6. Nanowire diameters versus HCl content of electrolyte corresponding to the four PL peaks. Detailed explanations are given in the text. $T=295$ K.

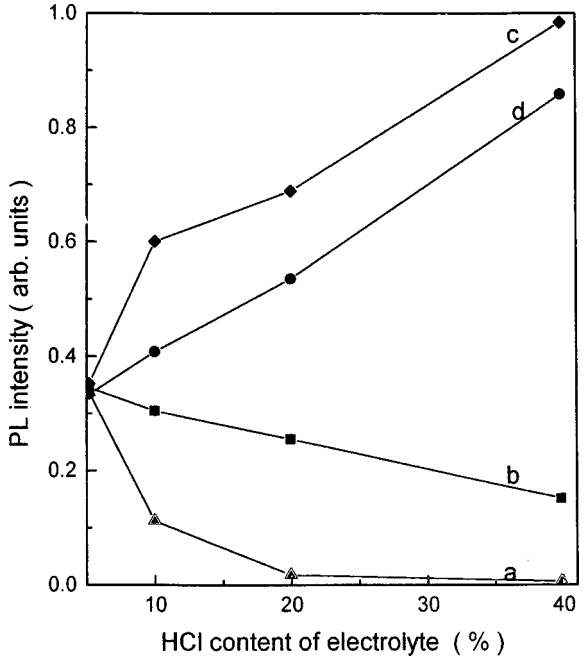

FIG. 7. Relative PL peak heights versus HCl content of electrolyte. $T = 295$ K.

the structural instabilities of the wirelike nanocrystallites of the PS samples.

To obtain similar structural information on our nonstandard samples, we have examined their PL spectra as a function of laser irradiation time. Figures 9–11 show the time evolution of the PL spectra of, respectively, samples $A2$, $A3$, and $A4$ under laser irradiation of 50 mW. For samples $A2$ and $A3$, the PL intensities and the line shapes vary with time. As the irradiation time increases, the intensities of all peaks

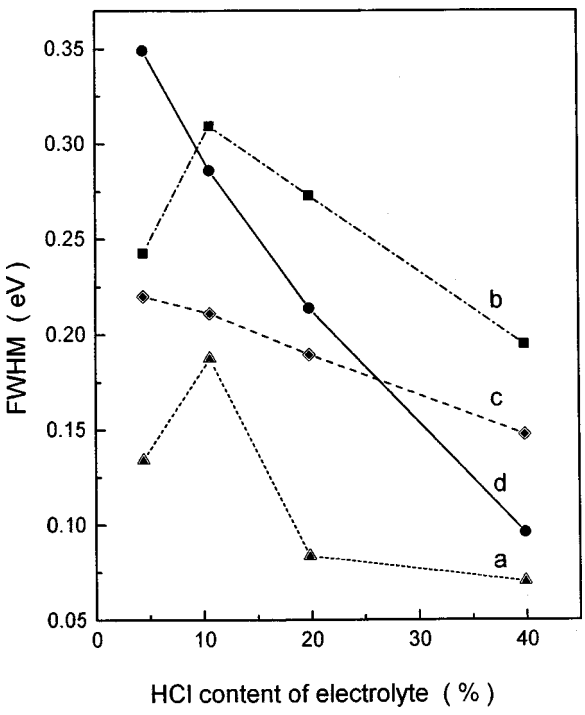

FIG. 8. PL peak widths versus HCl content of electrolyte. $T = 295$ K.

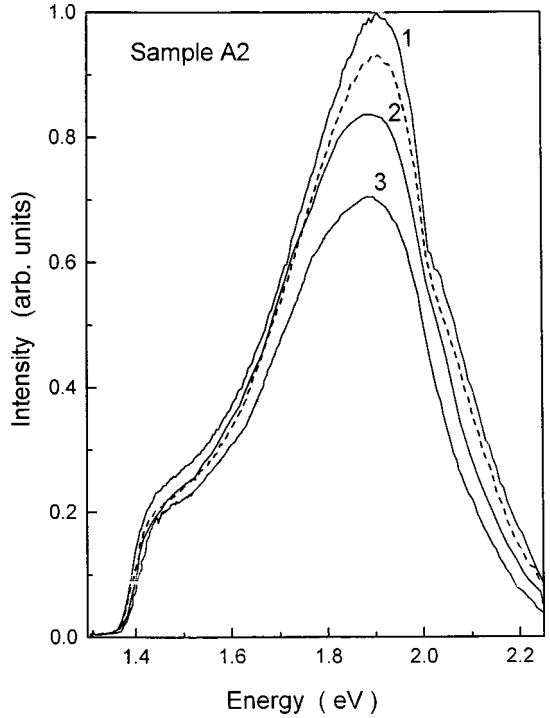

FIG. 9. PL spectra of sample $A2$ after laser irradiation for 0 (1), 30 (2), and 60 (3) min. Laser power 100 mW. The dashed curve shows the PL spectrum of the 60-min-irradiated sample $A2$ after depositing it for 2 h in the dark. Excitation wavelength and power are 488 nm and 100 mW, respectively. $T = 295$ K.

decrease monotonically for laser levels between 0.5 and 5 W cm^{-2}. Keeping the laser treated samples $A2$ and $A3$ in dark for two hours, their PL spectra recover, as seen in Figs. 9 and 10. Such behavior differs from that of sample $A1$ which irreversibly loses PL intensity in the low-energy region after irradiation, just like sample $A0$ does.[21–23] The irreversible changes for samples $A0$ and $A1$ may be attributed to the laser-induced oxidation of the nanocrystals of these PS samples, particularly, to the photoinduced oxidation of spongelike structures with substoichiometric oxides, SiO_x, on their surfaces. This oxidation, obviously, is absent in the case of samples $A2$ and $A3$. The reversible changes of the PL spectra of these samples are caused by local heating which thermalizes only slowly, due to the bad thermal conductivity of the spongelike layers which still exist for these samples. These conclusions are also supported by investigations of the PL spectra of samples $A1$,$A2$,$A3$ at low temperature ($T = 1.4$ K). The samples were mounted inside a volume filled with liquid helium and were exposed to laser irradiation of 50 mW and 100 mW power during 60 min. No changes of the PL spectra were observed. This is evidently due to the absence of oxygen in the chamber as well as to the effective cooling of the sample. In the case of sample $A4$ shown in Fig. 10, both the PL peak position and intensity are almost unchanged under laser irradiation for, at least, 40 min. This implies, in particular, that no local heating takes place, which is understandable since no spongelike layers of low thermal conductivity exist anymore. The absence of photoinduced oxidation for samples $A2$,$A3$,$A4$ means that the silicon wires have been covered by stable SiO_2 already during preparation.

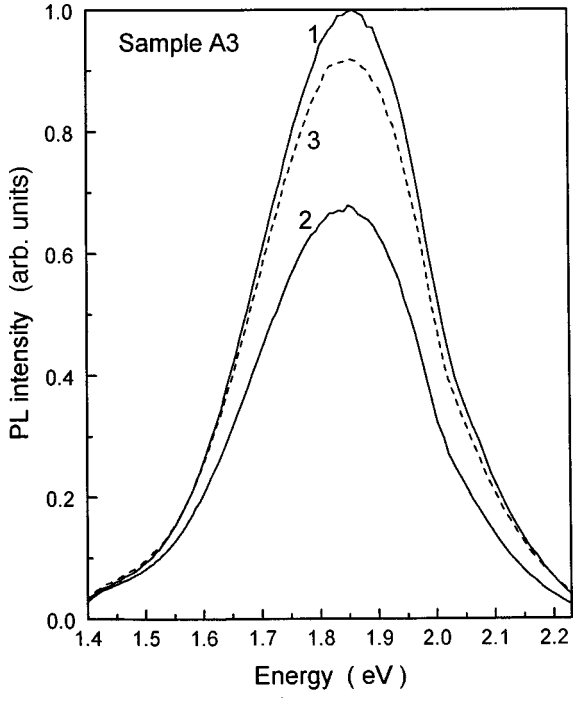

FIG. 10. PL spectra of sample $A3$ after laser irradiation for 0 (1) and 60 (2) min. Laser power 100 mW. The dashed curve (3) shows the PL spectrum of the 60-min-irradiated sample $A3$ after depositing it in dark for 2 h. Excitation wavelength and power as in Fig. 9. $T=295$ K.

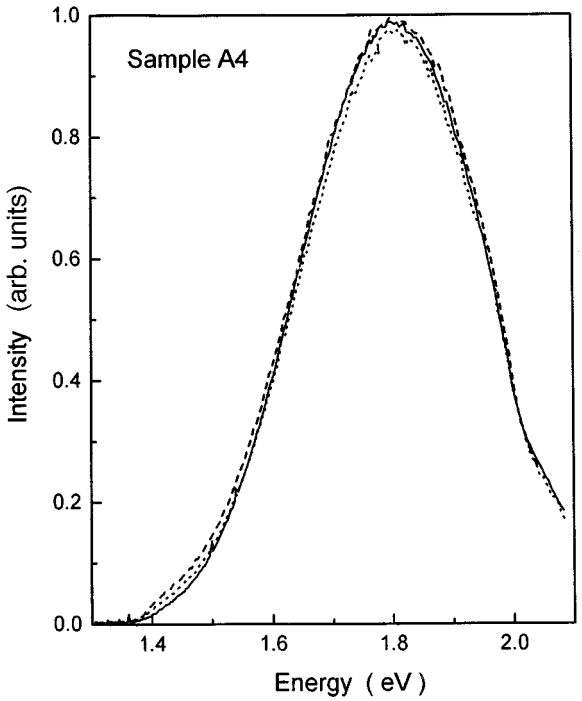

FIG. 11. PL spectra of sample $A4$ after laser irradiation for 0 (solid line), 30 (dashed line), and 60 (dotted line) min. Excitation wavelength and power as in Fig. 9. $T=295$ K.

V. CONCLUSIONS

The above experimental data on the PL spectra and their laser-induced changes give some hints why the new preparation procedure results in PS samples of much higher PL intensity and structural stability. It is generally believed that the kind of porosity of the samples is decisive for their PL properties.[20] If not enough silicon is removed during the anodization process, as in PS with low porosity, oxidation cannot proceed efficiently because oxygen cannot easily penetrate the internal region of PS to oxidize it. If, on the other hand, the evolution of pores is too rapid, the total wire surface increases too fast, making it difficult to fully oxidize the Si wires at room temperature. As a result, the wires are covered by substoichiometric silicon oxide. In our preparation process, obviously, the evolution of pores is neither too slow nor too fast, providing a wire structure rather than a sponge-like structure and a SiO_2 layer on the wire surfaces. The absence of Si dangling bonds, which would act as efficient nonradiative recombination centers,[17] could explain the intense luminescence of our PS samples, and also their stability against postanodization and exposition to air.

ACKNOWLEDGMENTS

This work has been supported by the Russian Fund for Basic Research (Grant Nos. 96-02-18853 and 95-02-04510) as well as by CNPQ and FAPESP (Brazilian funding agencies).

[1] L. T. Canham, Appl. Phys. Lett. **57**, 1046 (1991).
[2] S. S. Lyer and Y. H. Xie, Science **206**, 40 (1993).
[3] A. G. Gullis, and L. T. Canham, Nature (London) **353**, 335 (1991).
[4] H. Koyama, N. Shima, and N. Koshida, Phys. Rev. B **53**, R13 291 (1996).
[5] S. K. Deb, N. Mathur, A. P. Roy, S. Banerjee, and A. Sardesai, Solid State Commun. **101**, 283 (1997).
[6] P. D. J. Calcott, K. J. Nash, L. T. Canham, A. J. Simmons, and A. Loni, *Second International Conference on Low Dimensional Structures and Devices, Lisbon, 1997* [Mat. Sci. Eng. B] (to be published).
[7] R. Tsu, H. Shen, and M. Dutta, Phys. Lett. A **205**, 117 (1995).
[8] I. Gregora, B. Champagnon, L. Saviot, and Y. Monin, Thin Solid Films **255**, 117 (1995).
[9] S. L. Zhang, Y. T. Hou, and K. S. Ho, J. Appl. Phys. **72**, 4469 (1992).
[10] T. Suemoto, K. Tanaka, A. Nakajima, and T. Itakura, Phys. Rev. Lett. **70**, 3659 (1993).
[11] D. W. Zheng, Y. P. Huang, Z. J. He, A. Z. Li, T. A. Tang, R. Kwor, Q. Cui, and X. J. Zhang, J. Appl. Phys. **81**, 492 (1997).
[12] T. Ya. Gorbach, G. Yu. Rudko, P. S. Smertenko, S. V. Svechnikov, M. Ya. Valakh, V. P. Bondarenko, and A. M. Dorofeev, Semicond. Sci. Technol. **11**, 601 (1996).
[13] A. I. Belogorokhov, V. A. Karavanskii, and L. I. Belogorokhova, Fiz. Tekh. Poluprovodn. **30**, 1177 (1996) [Semiconductors **30**, 621 (1996)].
[14] H. D. Fuchs, M. Stutzmann, M. S. Brandt, M. Rosenbauer, J. Weber, A. Breitschwerdt, P. Deak, and M. Cardona, Phys. Rev. B **48**, 8172 (1993).

[15] S. Banerjee, Phys. Rev. B **51**, 11 180 (1995).
[16] C. Delerue, G. Allan, and M. Lannoo, Phys. Rev. B **48**, 11 024 (1993).
[17] T. Takagahara and K. Takeda, Phys. Rev. B **46**, 15 578 (1992).
[18] J. R. Proot, C. Delerue, and G. Allan, Appl. Phys. Lett. **61**, 1948 (1992).
[19] N. S. Averkiev, V. M. Asnin, I. I. Markov, A. Yu. Silov, V. I. Stepanov, A. B. Churilov, and N. E. Mokrousov, Pis'ma Zh. Eksp. Teor. Fiz. **55**, 631 (1992) [JETP Lett. **55**, 657 (1992)].
[20] X. L. Wu, F. Yan, X. M. Bao, S. Tong, G. G. Siu, S. S. Jiang, and D. Feng, Phys. Lett. A **221**, 261 (1996).
[21] M. A. Butturi, M. C. Carotta, G. Martinelli, L. Passari, G. M. Youssef, G. Ghiotti, and A. Chiorino, Solid State Commun. **101**, 11 (1997).
[22] X. L. Wu, F. Yan, M. S. Zhang, and D. Feng, Phys. Lett. A **117**, 205 (1995).
[23] E. Ribeiro, F. Cerdeira, and O. Teschke, Solid State Commun. **101**, 327 (1997).